Characterization of short-range heterogeneities in sub-congruent lithium niobate by micro-Raman spectroscopy

2006 J. Phys.: Condens. Matter 18 957

(http://iopscience.iop.org/0953-8984/18/3/013)

INSTITUTE OF PHYSICS PUBLISHING JOURNAL OF PHYSICS: CONDENSED MATTER

J. Phys.: Condens. Matter **18** (2006) 957–963 doi:10.1088/0953-8984/18/3/013

Characterization of short-range heterogeneities in sub-congruent lithium niobate by micro-Raman spectroscopy

Y Zhang[1,3], L Guilbert[1], P Bourson[1], K Polgár[2] and M D Fontana[1]

[1] Laboratoire Matériaux Optiques, Photonique et Systèmes, University of Metz and Supelec, UMR 7132 CNRS 2, rue E. Belin 57070 Metz, France
[2] Research Institute for Solid State Physics and Optics of the Hungarian Academy of Sciences, 1121 Budapest, Konkoly-Thege M.u.29/33, Hungary

E-mail: bourson@metz.supelec.fr

Received 19 July 2005
Published 6 January 2006
Online at stacks.iop.org/JPhysCM/18/957

Abstract

The spectral widths of Raman lines in nominally pure lithium niobate are measured as a function of the cationic molar ratio, in a wide range from stoichiometry (50 mol% Li) to sub-congruent compositions (below 48.6 down to 47 mol% Li). The broadening observed on the sub-congruent side follows the same slopes as on the congruent-to-stoichiometric side. It is shown that micro-Raman analysis permits one to characterize short-range heterogeneities at the micron scale, such as growth striations in bulk crystals or lithium out-diffusion in the surroundings of titanium-diffused waveguides, with a typical accuracy of 0.04 mol%.

1. Introduction

Because of its interesting electro-optical, photorefractive and nonlinear optical properties, lithium niobate ($LiNbO_3$, LN) covers a wide field of optical applications such as frequency doublers, parametric oscillators, holographic memories, and electro-optic components both in bulk form (Pockels cells) and integrated form (bidirectional couplers, switches, modulators). Light-induced phenomena (photoconductivity, photovoltaic effect, photorefractivity, photo-absorption, photoluminescence) usually appear either as key principles or as drawbacks depending on the application. In nominally pure LN, these phenomena mainly depend on the content of intrinsic defects [1, 2], which are related to the non-stoichiometric composition.

Furthermore, the fabrication process of integrated components on LN can induce out-diffusion of lithium from the sample [3]. In particular, optical devices based on LN:Ti waveguides usually exhibit an increased Li deficiency at the surface of the wafer, owing to the

[3] Present address: Physics Department, Southwest China University Chongqing, 400715, People's Republic of China.

high-temperature annealing process which is necessary for titanium in-diffusion. Hence the surface layer becomes sub-congruent, i.e. the Li/Nb ratio goes down below the congruent value. If not properly controlled, this process can result in lithium triniobate precipitates ($LiNb_3O_8$), with dramatic consequences on the guiding properties. It is thus useful to characterize Li out-diffusion at high spatial resolution.

The congruent composition, which is defined by the equal amounts of Li in the melt and in the crystal as well, depends on the crystal growth technique and is generally about 48.4–48.6%.

Several non-destructive methods can be used to measure the composition of pure LN, with typical accuracies ranging from 0.01 to 0.05 mol% [4]. Some of these methods (density measurements, NMR, EPR, second harmonic generation) require a specific shaping of the sample. Optical methods (UV absorption edge, refractive index and birefringence measurements) can work on polished LN wafers without further preparation, but with a rather poor spatial resolution ($\sim$20 μm). Up to now, only micro-Raman spectroscopy allows composition measurements with a spatial resolution in the micrometre range. Initially, Okamoto *et al* [5] compared and analysed the difference in the Raman spectra for two samples with congruent and stoichiometric compositions; some other works try to explain the phonon broadening of A1 and E symmetry modes [6].

Later, a linear relationship between the Li deficiency and the broadening of Raman peaks was established for compositions ranging from congruence to stoichiometry for the first time by Okamoto *et al* [5] and subsequently by several authors [7, 8]. However, accurate data in the sub-congruent range are still missing. Moreover, all these measurements have been made on macroscopic Raman with right angle experiments, incompatible with measurements of optical waveguides or surfaces. In addition, these experiments require large samples, whereas this is not the case with micro-Raman spectroscopy, where the analysed surface is of the order of a square micron, and these measurements do not require any preparation of the crystal.

In this paper, LN crystals of different compositions are studied by Raman spectroscopy in order to obtain the relationship between the full width at half maximum (FWHM) of Raman peaks and the composition, not only between congruence and stoichiometry, but also in the sub-congruent range. Then, the high spatial resolution of micro-Raman spectroscopy ($\sim$0.5 μm in the plane of observation) is used to characterize short-range heterogeneities along the growth axis of the sub-congruent Czochralski-grown crystal (growth striations) and near the surface of Ti-diffused samples.

2. Scaling of Raman spectroscopy to composition measurements

Nominally pure congruent and sub-congruent $LiNbO_3$ crystals were grown by the conventional Czochralski technique, whereas stoichiometric crystals were obtained by the flux technique from a mixture of $LiNbO_3$ and K_2O [9]. The composition of the crystals was determined by the UV absorption-edge method [10].

Raman experiments were performed using a Labram spectrometer (Jobin–Yvon) equipped with a 633 nm He–Ne laser, a confocal microscope and a CCD detector. The Stokes spectra were recorded at room temperature in the range 100–1000 cm^{-1}.

Figure 1 shows a typical Raman spectrum of pure congruent $LiNbO_3$ recorded in the Z(YX)Z configuration. The strong peak at about 152 cm^{-1} is E(TO1). According to the normal modes calculated by Caciuc *et al* [11] this peak corresponds to Nb/O vibrations. The line E(TO6) at about 365 cm^{-1} is attributed to Li/O vibrations. The line E(TO8) at about 580 cm^{-1} corresponds to the stretching vibration of the oxygen octahedron (O/O).

Figure 2 shows a spectrum in the Y(ZZ)Y configuration. According to Caciuc *et al* [11] the line A1(TO1) corresponds to Nb/O vibrations, A1(TO2) mainly involves Li/Nb motions, whereas A1(TO3) and A1(TO4) correspond to distortions of the oxygen octahedron.

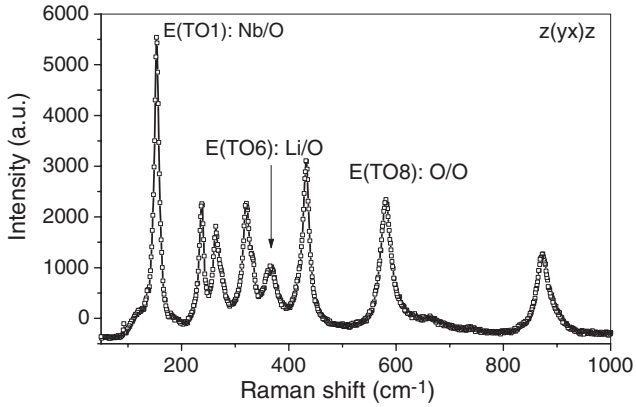

Figure 1. Typical Raman spectrum of pure congruent $LiNbO_3$ in the Z(YX)Z configuration. E(TO1) is attributed to Nb/O vibration, E(TO6) to Li/O vibration. (Acquisition time: 30 s per point.)

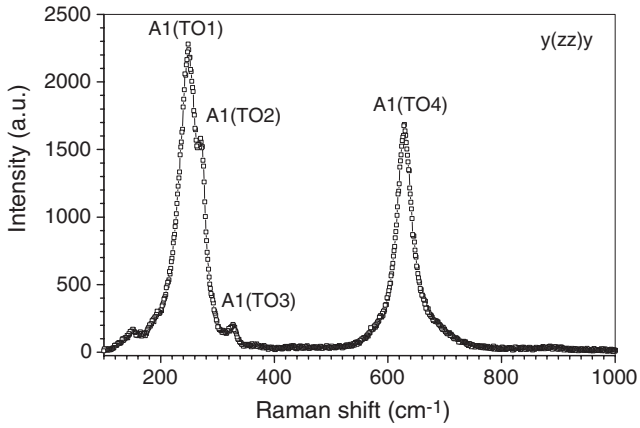

Figure 2. Typical Raman spectrum of pure congruent $LiNbO_3$ in the Y(ZZ)Y configuration. A1(TO1) is attributed to Nb/O vibration. (Acquisition time: 5 s per point.)

The widths of the Raman peaks indicate disorder within the crystal structure. In particular, the widths of E(TO1) and A1(TO1) are specially interesting because they are thought to reflect the disorder in the Nb sub-lattice (assuming that oxygen sites are fully and normally occupied). In the back-scattering configuration used for the micro-Raman experiments, E(TO1) is visible in z-cut samples, whereas A1(TO1) can be used in x-cut or y-cut samples. Previous studies have established linear dependences of the full width at half maximum (FWHM) of these two Raman lines as a function of the composition from congruence to stoichiometry [5, 7, 8, 12, 13]. As shown in figures 3 and 4, the results obtained in the present work in the same range of composition confirm these previous results, and moreover they show that the slopes remain unchanged in the sub-congruent range, at least until the Li content $X_c = 46.98$ mol%. Linear fittings give the full width at half maximum Γ (cm^{-1}) versus X_c (mol%) and vice versa:

$$\Gamma_{E(TO1)} = 5.54 + 4.313\ (50\% - X_c) \qquad X_c = 51.28 - 0.232 \times \Gamma_{E(TO1)}$$

$$\Gamma_{A1(TO1)} = 18.00 + 8.086\ (50\% - X_c) \qquad X_c = 69.39 - 0.123 \times \Gamma_{A1(TO1)}.$$

Note that these formulae involve the instrumental linewidth, $\sim$0.2 cm^{-1} in our experiments.

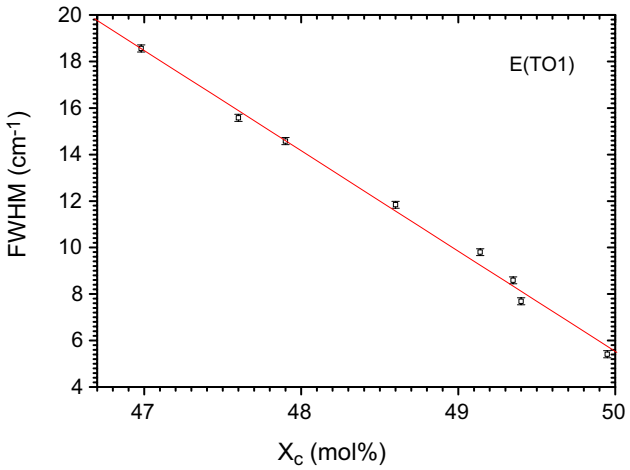

Figure 3. FWHM of E(TO1) as a function of lithium niobate composition. The Li_2O content in the crystal (mol%) was determined from the UV absorption edge.

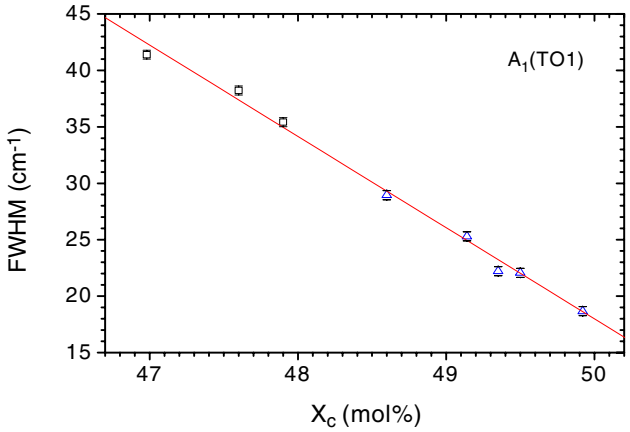

Figure 4. FWHM of A1(TO1) as a function of lithium niobate composition. The Li_2O content in the crystal (mol%) was determined from the UV absorption edge.

In the same measurement conditions, the line A1(TO1) is more intense than E(TO1), and the slope $\Gamma_{\mathrm{A1(TO1)}} = f(X_c)$ is about twice the slope $\Gamma_{\mathrm{E(TO1)}} = f(X_c)$. Hence, the method should be in principle more sensitive in x-cut or y-cut samples than in z-cut samples. However, A1(TO1) is less easy to fit because it is close to A1(TO2). That is why the standard error on Γ given by the fitting procedure is always larger for A1(TO1) (about 0.3 cm^{-1}) than for E(TO1) (about 0.15 cm^{-1}). Finally, the accuracy of the composition determined by Raman spectroscopy is almost the same, ∼0.04 mol%, independently of the line used. In comparison, the UV absorption edge [4] is more accurate (∼0.02 mol%), but being a volumic method it gives an integrated value over the measured volume. The big advantage of micro-Raman spectroscopy is, of course, 3D resolution. Now we show the capability of this technique for recording short-range heterogeneities related to growth striations in as-grown crystals or to lithium out-diffusion in annealed samples.

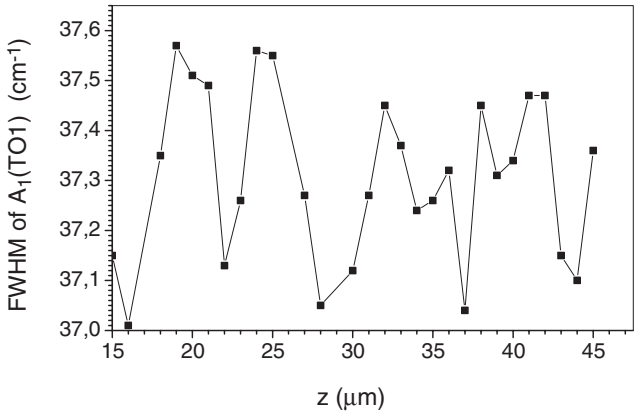

Figure 5. Horizontal scan of the FWHM of A1(TO1) along the growing axis z of a Czochralski-grown sub-congruent crystal. The sample was cut perpendicular to y.

3. Recording short-range heterogeneities by micro-Raman analysis

For all micro-Raman experiments, the incident wavelength was 633 nm, the objective magnification was 100 and the confocal hole diameter was 300 μm. In these conditions, the spatial resolution is about 0.5 μm in the plane and 1.3 μm along the vertical axis of the set-up (in air). Taking account of the refractive index of LN, the axial resolution in the sample is about 3 μm.

3.1. Growth striations in an as-grown sub-congruent crystal

The middle part of the sub-congruent LN crystal used in the scaling experiments was cut along the (zx) plane containing the growth axis z. Figure 5 shows the FWHM of A1(TO1) recorded along the z-axis, by steps of 1 μm. Short-range heterogeneities, roughly periodic, are observed. The period along z is about 5–7 μm, and the amplitude of variation of the FWHM is $\sim$0.6 cm^{-1}, which is two times larger than the standard error given by the fitting procedure. The observed quasi-periodic variations can thus be attributed to growth striations. According to the previous scaling (figure 4), the corresponding amplitude of LN composition variations along the growing axis of this sub-congruent Czochralski-grown crystal would be about 0.07 mol%. It could be interesting to perform the same kind of experiment in a quasi-stoichiometric crystal, in order to check whether short-range inhomogeneities related to growth striations are also visible by this technique when the crystal is grown from a Li-rich melt.

3.2. Lithium out-diffusion in a titanium-diffused sample

Titanium-diffused channel waveguides have been fabricated on a congruent z-cut wafer. The sample was annealed under wet argon atmosphere at 1027 °C for 12 h. The FWHM of E(TO1) was recorded as function of depth, out of across the waveguides, by moving the sample vertically by steps of 0.5 μm. The result is shown in figure 6. Zero depth corresponds to the surface, and the actual depth is obtained by multiplying the mechanical displacement by the ordinary refractive index (2.28 at 633 nm). The FWHM at the surface is significantly larger than it is in bulk. Hence, the surface layer is sub-congruent, as a consequence of lithium out-diffusion during the annealing process at high temperature. Using the previous scaling

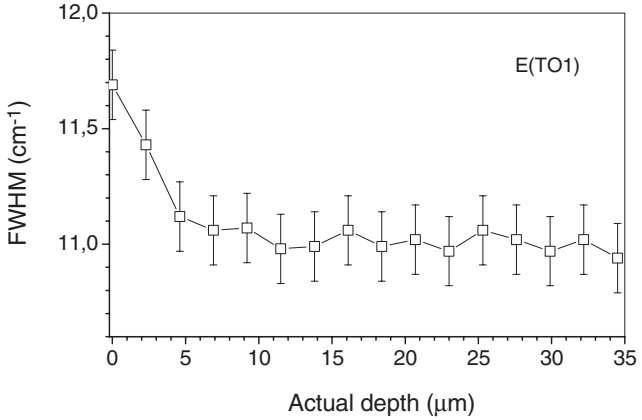

Figure 6. Vertical scan of the FWHM of E(TO1) along the z-axis perpendicular to the surface of a titanium-diffused waveguide. The actual depth is determined by multiplying the mechanical displacement by the ordinary refractive index.

(figure 3), it can be estimated that the Li deficiency at the surface has increased by at least 0.14 mol% compared to the bulk. When optimizing waveguide fabrication, routine micro-Raman characterization could be useful after Ti diffusion, at least each time the annealing conditions or the wafer preparation are changed within the fabrication process. Vertical scans would give a fairly good estimation of lithium out-diffusion at the surface [14]. However, the exact profile versus depth is more difficult to estimate, because the axial resolution ($\sim$3 μm) here is not small compared to the depth of the profile ($\sim$6 μm). For this reason, the surface loss of 0.14% Li here above reported is probably a lower estimate.

4. Conclusion

The spectral widths of E(TO1) and A1(TO1) Raman lines have been shown to be a good calibration of lithium niobate composition. The Raman method has been scaled relatively to the UV-absorption method by using as-grown samples. Linear dependences of the spectral widths E(TO1) and A1(TO1) on LN composition have been confirmed in a wide range of practical interest, extending from 47% (sub-congruent) to 50% (stoichiometric). The typical accuracy of the method was found to be $\sim$0.04 mol% for both Raman lines. Using these scalings, micro-Raman spectroscopy can be a powerful, non-destructive tool for the characterization of short-range constitutional heterogeneities, such as growth striations in Czochralski crystals, or lithium out-diffusion in titanium-diffused samples, within the spatial resolution of confocal microscopy ($\sim$0.5 μm $\times$ 0.5 μm $\times$ 3 μm).

Acknowledgments

This research was partially supported by The National Fund for research of Hungary (OTKA) under contract No T-034176, the region Lorraine and the French Ministry of Research on the framework CPER programme. The first author is also supported by the Natural Science Foundation of Chongqing (Grant No CSTC 2005BB4047) and by SRF for ROCS, SEM-Grant No 2005 38.

References

[1] Abrahams S C and March P 1986 *Acta Crystallogr.* B **2** 61–6
[2] Lerner P, Legras C and Dumas J P 1968 *J. Cryst. Growth* **3** 231
[3] Smyth D M 1983 *Ferroelectrics* **50** 93–102
[4] Wöhlecke M, Corradi G and Betzler K 1996 *Appl. Phys.* B **63** 323–30
[5] Okamoto Y, Wang P-C and Scott J F 1985 *Phys. Rev.* B **32** 6787–92
[6] Anikiev A, Reznik L G, Umarov B S and Scott J F 1985 *Ferroelectr. Lett.* **3** 89–96
Scott J F, Halliburton L E, Kanata T, Kovacs L, Skvortsov A P, Thomson P D, Foldvari I and Kubota K 1989 *Properties of Lithium Niobate* (*EMI Datareviews Serie 5*) (London: INSPEC) pp 169–204
[7] Schlarb U, Klauer S, Wesselman M and Wöhlecke M 1993 *Appl. Phys.* A **56** 311–26
[8] Ridah R, Fontana M D, Bourson P and Malovichko G 1997 *J. Phys.: Condens. Matter* **9** 9687–93
[9] Polgár K, Péter A, Kovács L, Corradi G and Szaller Z 1997 *J. Cryst. Growth* **177** 211
[10] Földvári I, Polgár K, Voszka R and Balasanyan R N 1984 *Cryst. Res. Technol.* **19** 1659–61
[11] Caciuc V, Postnikov A V and Borstel G 2000 *Phys. Rev.* B **61** 8806–13
[12] Malovichko G I, Grachev V G, Kokanyan E P, Schirmer O F, Betzler K, Gather B, Jermann F, Klauer S, Schlarb U and Wöhlecke K 1993 *Appl. Phys.* A **56** 103–8
[13] Abdi F, Aillerie M, Bourson P, Fontana M D and Polgar K 1998 *J. Appl. Phys.* **87** 2251–4
[14] Zhang Y, Guilbert L and Bourson P 2004 *Appl. Phys.* B **78** 335–61